

---

## EPITHERMAL GOLD OCCURRENCES IN THE LAKES DISTRICT OF THE MAIN ETHIOPIAN RIFT AND TENDAHO AREA OF THE AFAR RIFT: DISCOVERY OF A METALLOGENIC PROVINCE

Solomon Tadesse

Department of Geology and Geophysics, Faculty of Science, Addis Ababa University, PO Box 1176, Addis Ababa, Ethiopia, E-mail: dgg@telecom.net.et

**ABSTRACT:** Plio-Quaternary volcanic products cover a large part of the Main Ethiopian Rift (MER). Epithermal gold occurrences related to Quaternary volcanics are at present being closely studied for their precious metal potential. Low sulphidation (Adularia-sericite-type) occurrences have been found. Analyses of 579 core and cutting samples collected for the purpose of exploratory geothermal studies from a number of localities (Gedemsa, Aluto and Corbetti calderas MER, and the Tendaho graben; Afar) were analyzed for gold. The results showed concentration of gold ranging from 100 ppb to 440 ppb. Values ranging between 200 and 300 ppb are very common. The overall characteristics of the known ore occurrences and the evolution of the Quaternary central volcanoes within the MER, and related epithermal processes seem to delineate an individual, homogeneous metallogenic province. A new field of investigation on epithermal ore occurrences which are unusual for the present Ethiopian metallogenic scenery is probably emerging. A study of these phenomena, in light of recent acquisitions in metallogenic knowledge, could be of interest not only for further scientific studies but also for new possibilities in mining activity. This study presents the occurrences of epithermal gold mineralization in the MER, the only one of its kind so far reported in the East African Rift System.

**Key words/phrases:** Caldera, epithermal gold, metallogeny, Plio-Quaternary, rift volcanics

### INTRODUCTION

Epithermal precious metal mineralization is commonly associated with Cenozoic geothermal systems in areas of calc-alkaline volcanism. Much of this volcanism typically occurs above subduction zones along continental margins and in island arcs as well as along spreading mid-ocean ridges (*e.g.*, Burke *et al.*, 1981;

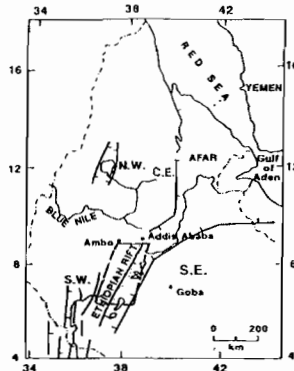
Harris *et al.*, 1986). Less commonly, economic mineralization may be associated with continental rift zones, such as the extensive rift system that cuts through south-western Asia and continues along the eastern side of Africa. This system already includes sectors that represent evolving oceanic basins (the Gulf of Aden and the Red Sea), but mostly it is comprised of subaerial intracratonic rifts, including the Ethiopian Rift Valley. Subaerial volcanism in the Ethiopian Rift Valley has caused hydrothermal activity, which is still active in several sites being investigated for geothermal energy. Extinct geothermal fields are also quite common. The possibility that these geothermal systems, related to the continental rifting, have been and may be ore-forming systems cannot be discarded a priori.

The Ethiopian Rift Valley in general held little more than an academic interest in scientific circles for a long period of time. Detailed geological studies and regional mapping of the rift valley have been conducted during the last 29 years (Di Paola, 1972). These have helped delineate specific industrial resources (*e.g.*, diatomite, bentonite, soda ash and geothermal steam), mainly through the work of the Ethiopian Institute of Geological Surveys. Studies aimed at identifying epithermal-type precious metal (mainly gold) resources within the Ethiopian Rift are relatively recent. The present work reports preliminary observations at selected sites within the Ethiopian Rift Valley and Afar where gold anomalies that are clearly associated with rift volcanism have now been found.

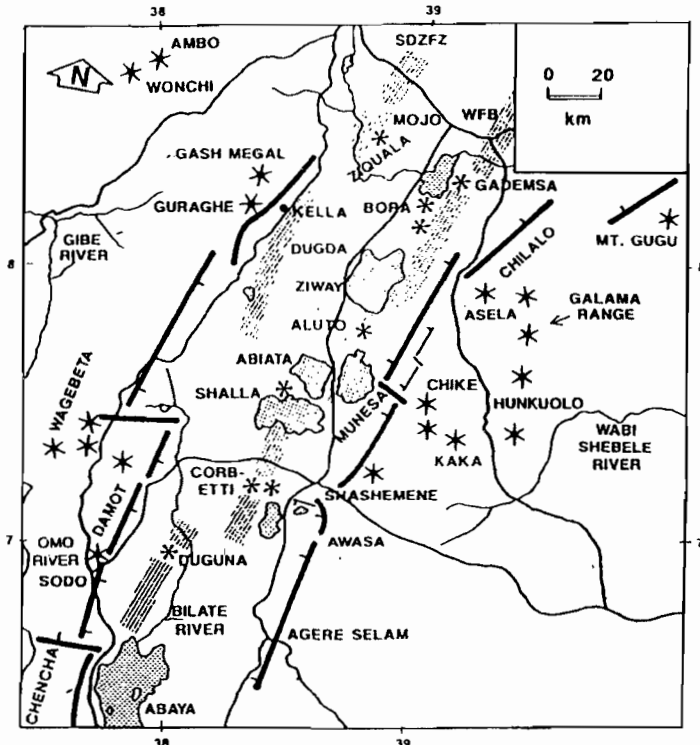
## REGIONAL GEOLOGY OF THE ETHIOPIAN RIFT AND AFAR

The Ethiopian Rift is the northern most extension of the great East African Rift that extends from north-eastern Ethiopia to Mozambique in southern Africa, with a length of more than 4000 km. More than one-quarter of the rift system lies in Ethiopia (Fig. 1). The Ethiopian Rift is a large 1 km deep graben with an average width of about 70–80 km and a length of 700 km stretching from the Ethio-Kenyan border in the south to the Afar Depression in the north. The rift dissects the highlands of the country into the eastern and western plateaus and is bounded on two sides by a series of large normal (step) faults (Fig. 1). The eastern escarpment of the MER is characterised by step faults with significant throws in its northeastern sector exceeding 1500 m between the top of the plateau and the rift floor. The western margin is gradational and less marked thus accounting for the asymmetry of the MER. Continuous tectonic movements are confirmed by numerous young faults affecting Holocene rock units and by the intense seismicity of the whole region (Di Paola, 1972; Giday Woldegabriel *et al.*, 1990).

a)



b)



**Fig. 1. a)** Location of the Ethiopian and Afar rifts. **b)** The central sector of the MER and adjacent areas (modified after Giday Woldegabriel *et al.*, 1990). (Thick line segments represent rift margin faults with ticks on the downthrown side. Pointed stars represent rift-shoulder central volcanoes, and asterisks are Quaternary peralkaline rhyolite centres of the rift axis. The dual marginal Quaternary rift axes on the rift floor of the northern part of the central sector of the MER are expressed by tightly defined lines. Lakes are dotted, fine lines are rivers, and medium lines are major roads.)

The Ethiopian plateaus bordering the rift consist of a thick succession of flood basalts and subordinate amounts of rhyolites emplaced during Oligocene (Giday Woldegabriel *et al.*, 1990). The floor of the rift is commonly covered by Plio-Quaternary volcanic products and basin-fill volcanoclastic sediments. Basaltic volcanic rocks become progressively younger northwards to Afar, although young basaltic volcanism of minor volume is also common along the axial zone of the Ethiopian Rift. The main petrological feature of the MER is the abundance of silicic peralkaline volcanics (mainly pantallerites) related both to the fissural activity and to the several volcanoes rising from the rift floor. It has been suggested that east-west structures may be an important factor in controlling the locations of volcanism along the rift. Thick sediment accumulations of lacustrine origin cover large areas of the rift floor.

### **GEOLOGICAL SETTING AND EPITHERMAL MINERALIZATION OF THE PROSPECTING AREAS**

A reconnaissance study of epithermal mineralization within the central sector of the Main Ethiopian Rift Valley has been conducted since 1997. Several central volcanoes are present along the axial portion of the rift and two of these, Corbetti and Gedemsa, were studied in detail because of the relatively abundant available bore hole data and better accessibility of the areas.

The Aluto volcanic complex is a Quaternary volcanic centre located along the Wonji Fault Belt (WFB) in the central sector of the MER. The Tendaho graben is found further north in the Afar depression. The evolution of associated calderas at Gedemsa, Aluto, and Corbetti is attributed to central-type eruptions, with subsequent volcano-tectonic collapses.

Epithermal mineral occurrences have been observed in these four localities (Corbetti, Gedemsa, Aluto and Tendaho). Associated features are found on the surface and at depth in drill core. These include alteration patterns that display characteristic low sulphidation type epithermal occurrences. The low sulphidation alteration commonly displays a broad propylitized (chlorite, epidote, quartz) area that envelopes a core of pervasive potassic alteration, together extending to as much as several kilometres. Locally, intermediate argillic alteration assemblages commonly overprint the potassic alteration. The alteration zone also displays broad propylitic zones, overprinted by advanced

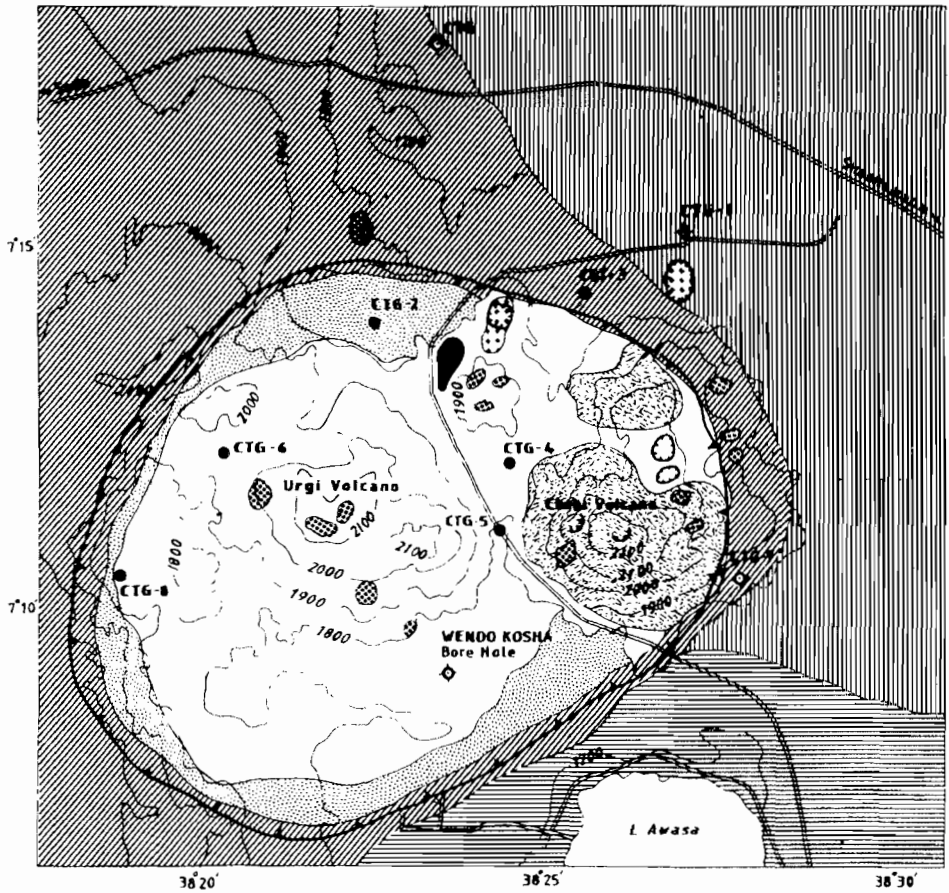
argillic alteration (kaolinite). Mineral phases include chlorite, kaolin, calcite, quartz and epidote, adularia, iron oxides, smectite and albite.

### ***The Corbetti caldera***

Corbetti is a Holocene volcanic complex found in the central sector of the MER. The most abundant volcanic rocks are peralkaline pyroclastics (ignimbrite and pumice) which are attributed to central-type eruptions with subsequent volcano-tectonic collapse (Di Paola, 1972). The geometric outline of the resulting caldera is elliptical with its long axis measuring about 12 km. The wall of the caldera has a variable height between about 50 m and 200 m.

Post-caldera activity is represented by the emplacement of two very recent volcanic centres (Urji and Chabbi) (Fig. 2) situated on active faults that parallel the major structural zone of the rift system. The Urji and Chabbi centres have extended unwelded pumice flows and falls with minor obsidian flows. Both centres are at fumarolic stage. Several NNE trending minor normal faults cut all the volcanic rocks except the youngest products of the Urji and Chabbi centres. Eight shallow tempograd bore holes have been sunk at different locations in and outside the caldera ranging in depth from 50–200 m (Fig. 2). The bore holes were irregularly located but have enabled constructing shallow subsurface volcanic stratigraphy (Fig. 3).

The Corbetti caldera appears to be one of the most economically promising among the newly discovered occurrences. Altered rock forms a roughly north-south elongated area some two kilometres long and several hundred meters wide. Steam activity is apparent only along the extremities of this zone, but it is possible that thick soil cover may have masked the rest of the area. A low sulphidation (Adularia-sericite type) alteration processes are indicated by propylitic and advanced argillic assemblages in ignimbrite, pumice and rhyolite. The alteration is characterised by the presence of chlorite, kaolin, calcite and quartz. The metallic minerals found in the shallow drill-chip samples include Fe- and Ti-oxides, sulphide minerals including pyrite and chalcopyrite and possibly Pb-bearing sulphosalts. The propylitic alteration, which is largely overprinted by later intermediate argillic alteration, surrounds an elongated and discontinuous core of potassic alteration. Advanced argillic alteration is limited to areas in proximity to the vents. Crusts of salts and silica occur around the vents. Some of these salts are greenish in colour and appear to be ferrous iron and copper. Weakly developed surface alteration zones locally occur, with Fe and Ti-oxide.





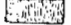









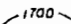



- Lithology:**
-  , Lacustrine deposits;
  -  , Pumice and detritus;
  -  , Obsidian lava flows;
  -  , Recent pumice flows and falls;
  -  , Old layer pumice;
  -  , Basaltic flows and scoria cones;
  -  , Ignimbrites;
  -  , Alterations.
- Topography:**
-  , CTG drill holes analyzed;
  -  , Other drill holes;
  -  , Crater;
  -  , Corbetti caldera outer rim;
  -  , Contour;
  -  , All weather road;
  -  , Lake;
  -  , Steaming ground.

Fig. 2. Geological sketch map of the Corbetti area (modified after Di Paola, 1972).

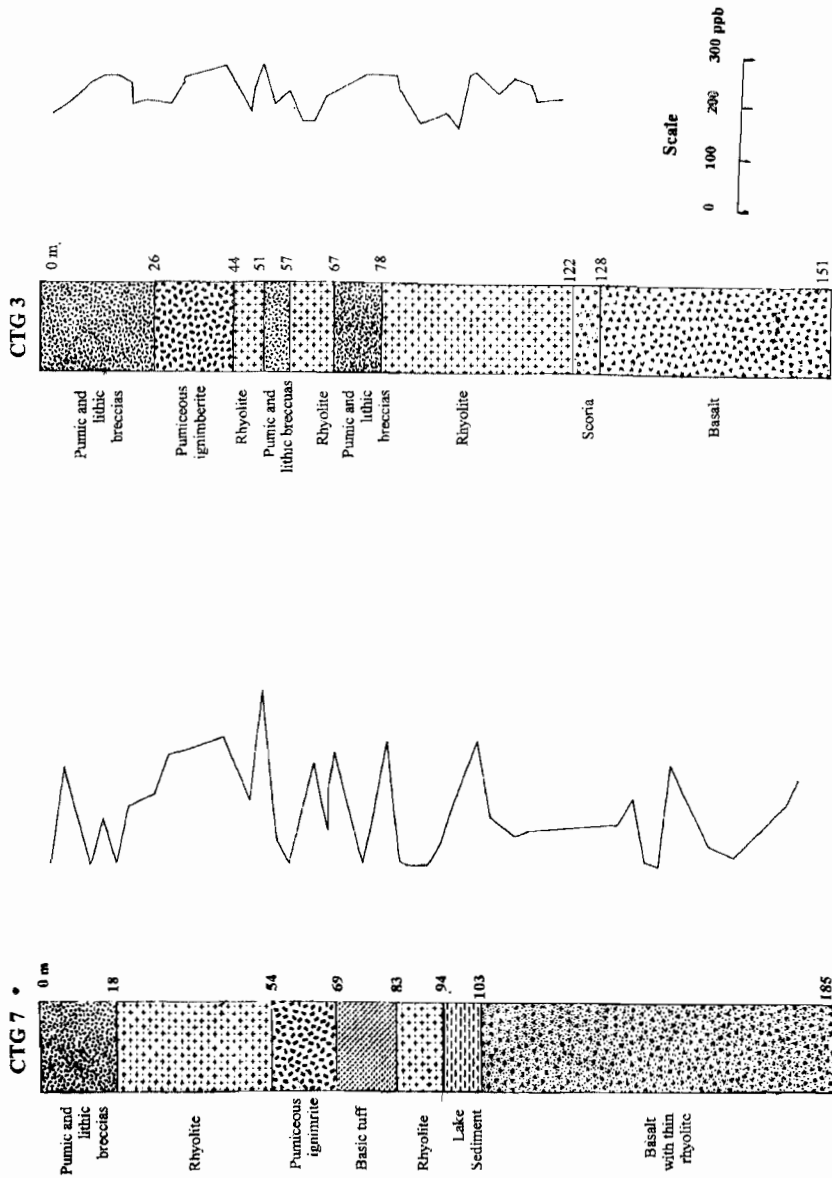
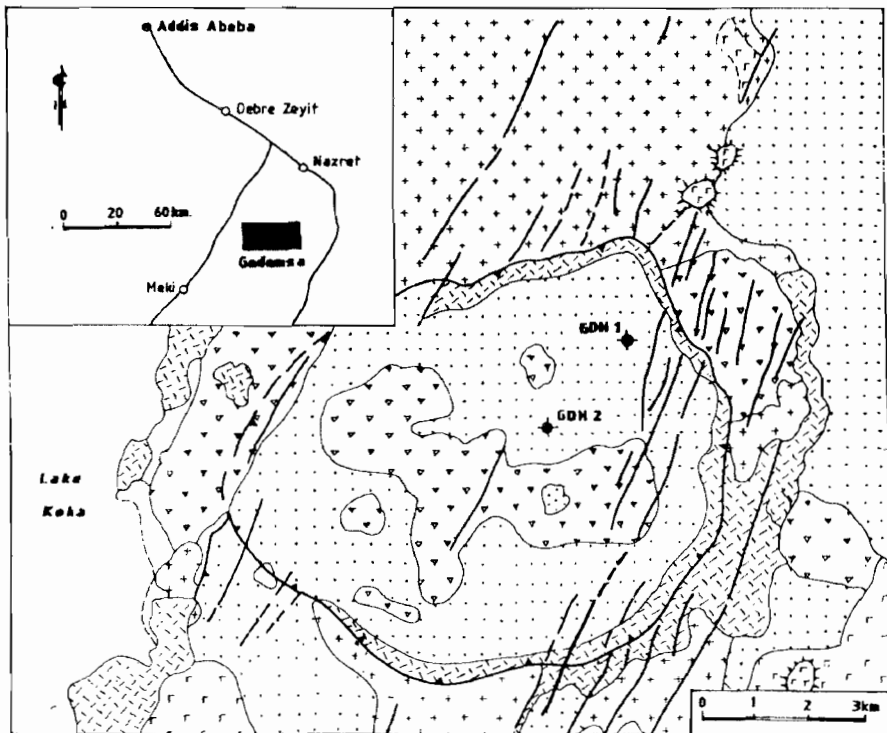


Fig. 3. Lithological columns of drill hole CTG-3 and CTG-7 with graph showing Au grade distribution.

### *Gedemsa caldera*

Gedemsa is a recent (0.8 to 0.1 Ma) volcano in the central sector of the MER (Fig. 4). The lowest exposed products consist of acidic lavas, which in turn are covered by thick plinian unwelded pumice fall deposits. The pumice deposits are overlain by an ignimbrite sheet. Basic surge deposits are found lying on the ignimbrite in the northern part of the volcano. Postcaldera activity has resulted in the emission of acidic lava and interbedded pyroclastic products within the caldera itself. The volcanic products of Gedemsa consist mainly of peralkaline trachytes and rhyolites, mafic rocks being represented only by inclusion occurring within some of the post-caldera products (Peccerillo *et al.*, 1995).



[Dotted pattern], Alluvium; [Cross-hatched pattern], Recent basaltic flows; [Triangular pattern], Post claderic pyroclastics and lava domes; [Wavy pattern], Rhyolitic lava flows and domes; [Plus sign pattern], Gedemsa ignimbrite and pyroclastics; [Solid line], Caldera rim; [Dashed line], Faults; [Sun-like symbol], Scoria cones.

**Fig. 4.** Geological sketch map and bore hole location of Gedemsa geothermal prospect (modified from Solomon Kebede, 1987).



The caldera itself is clearly a composite structure that resulted from repeated collapses following large plinian pyroclastic eruptions. The geometry of the caldera is almost circular, measuring about 10 kilometres in diameter. The whole caldera structure is strongly affected by many large closely-spaced NNE-SSW trending faults, especially at its eastern part. These faults belong to the Wonji Fault Belt and manifest active tectonics within the rift. Evidence for past hydrothermal activity is observed in the north-west caldera wall and on a small dome inside the caldera. Occurrences of several active thermal manifestations are also known along NNE fault lines immediately outside the caldera proper. The fossil manifestations have oxidised pumiceous deposits with some deposition of silica. Two shallow temperature gradient wells have been drilled within the Gedemsa caldera (Fig. 5) reaching depths of 190 and 200 meters, respectively with rock cutting samples taken every 3 meters.

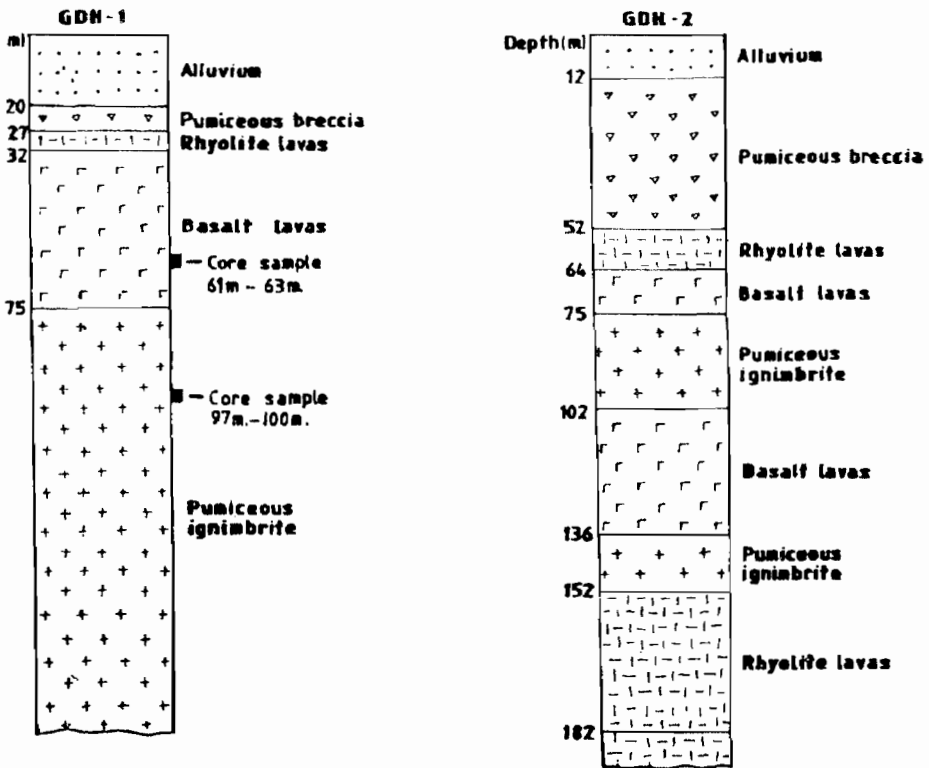


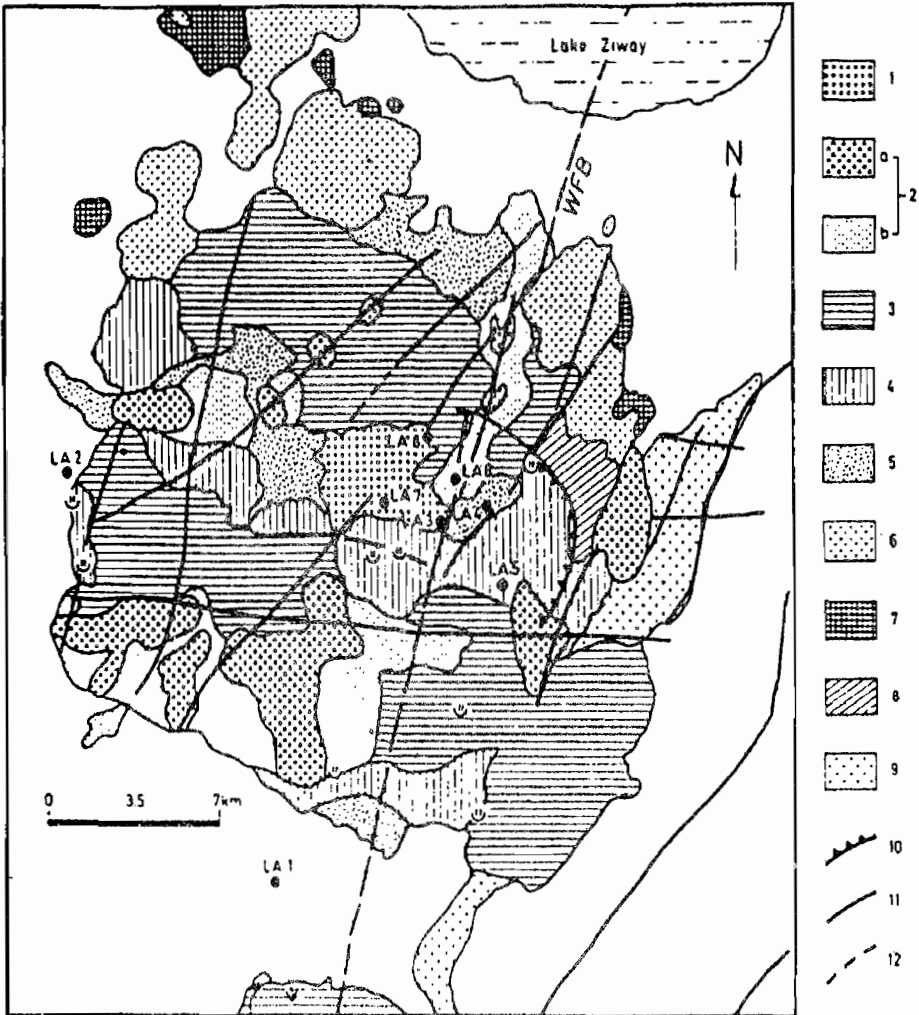
Fig. 5. Geological section in GDH-I and GDH-2 (Gedemsa caldera).

### *Aluto volcano*

The Aluto volcanic complex is a Quaternary volcanic centre located along the Wonji Fault Belt in the central sector of the MER (Fig. 6). The geology of this complex is relatively well-known from surface mapping supplemented by data on the deep stratigraphy and structure from eight deep exploratory wells (Fig. 7) that were sunk to depths ranging from 1300 to 2500 m.

According to Gianneli and Meseret Teklemariam (1993) the oldest outcropping rocks in the area are found at the adjacent eastern rift escarpment and consist mainly of silicic volcanics commonly known as the Tertiary ignimbrite unit. This unit is overlain by a fissural basaltic unit known as Bofa basalt, which in turn is covered by sediments of lacustrine origin that extend over large areas of the rift floor. The volcanic products of Aluto volcanic centre itself consist of a succession of ash-flow tuffs, silicic tuff breccias, silicic domes and unwelded pumice flows. These volcanic products are very young and are associated with surface thermal manifestations that consist of hot springs and fumaroles with temperatures up to 95° C, steaming grounds, silica sinter and travertine deposits. The hydrothermal deposit temperatures measured in the deep exploratory wells range from 88 to 335° C (Gianneli and Meseret Teklemariam, 1993).

The alteration observed in the studied samples from Aluto include an upper facies characterized by intermediate and propylitic assemblages. Intermediate argillic facies are typically represented by smectite group clay minerals; alteration intensity is variable, from incipient groundmass argillification to almost pervasive metasomatism. The latter is best developed in rock units originally very rich in glass. Propylitic alteration includes the characteristic minerals, calcite, chlorite, adularia, quartz and epidote. The metallic minerals found in the studied samples mostly include oxides and sulphides. The oxides consist of magnetite, ilmenite, hematite and Ti-oxide. The sulphide minerals are pyrite, chalcopyrite, sulphosalts possibly Pb. Pyrite is the most abundant.



**Fig. 6. Geological map, deep well (LA) location and thermal manifestations of the Aluto-volcano.** Legend: 1, Alluvial deposits; 2, Peralkaline rhyolite (a) and pumice (b); 3, Peralkaline rhyolite dome; 4, Rhyodacite dome; 5, Awarfu ignimbrite; 6, Rhyolite; 7, Hyaloclastite; 8, Collapsed pre-Aluto volcano; 9, Bofa Basalt; 10, Caldera rim; 11, Faults; 12, Inferred faults; WFB, inferred wonji fault belt (after ELC, 1986).

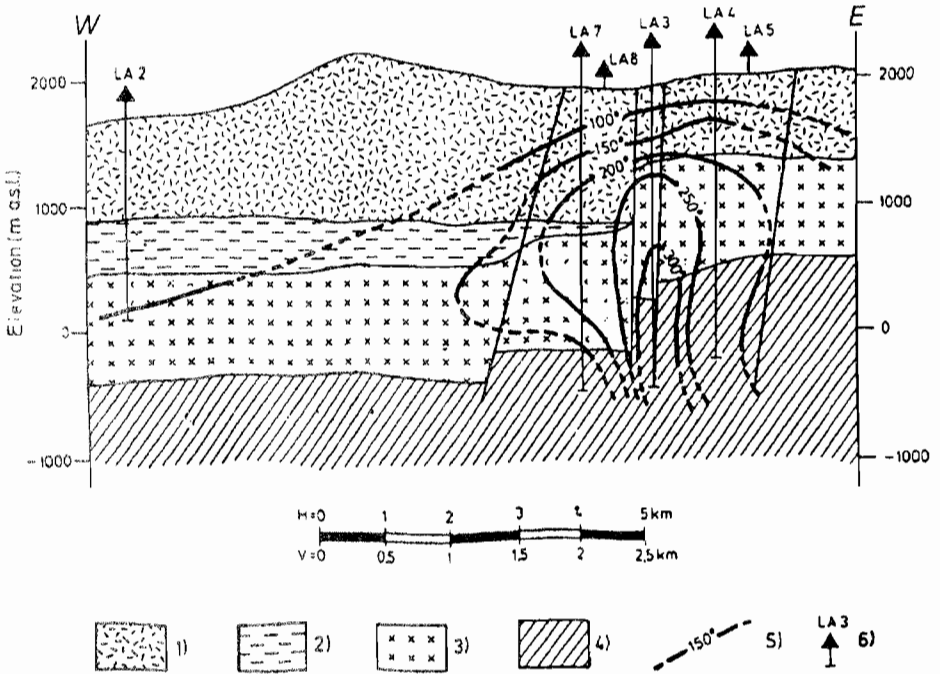


Fig. 7. E-W geological cross-section across Aluto volcano (after ELC, 1986). (1, Ignimbrite; 2, Peralkaline rhyolite; 3, Bofa basalt; 4, Collapsed per-aluto volcano; 5, Temperature gradient; 6, Bore hole number.

Gedemsa caldera is the northernmost studied area in the MER where epithermal mineralization occurs. Rhyolite lavas, ignimbrite and pumice deposits represent the host rocks. The alteration belongs to the low sulphidation type. This area appears to be the most promising among the low sulphidation occurrences. The alteration forms a roughly NW elongated area some 5 km long and several hundred metres wide. Propylitic alteration, which is largely affected by later intermediate argillic alteration, surround the zone of potassic alteration. Several thin quartz adularia veinlets cut the zone of potassic alteration. The occurrences are formed of crust form quartz and granular quartz. Carbonates and clay minerals are also present. The ore mineral assemblage includes pyrite, chalcopyrite, enargite, iron oxide minerals, epidote, chlorite and gold. In the western part of the caldera, pyrite occurs in fractured propylitized rhyolite, with narrow zones of potassic alteration and development of intermediate argillic

alteration. In the fractures, thin veins of cavernous quartz with abundant copper sulphide dissemination occur.

### ***The Tendaho graben***

This graben is found further north in the Afar Depression. It is a NW-SE trending graben about 50 km wide and is the southern extension of the Afar active spreading zones where the active Erta Ale-Manda Hararo volcanic ranges are situated. The Afar axial ranges are considered to be the exposed equivalents on land of the Red Sea oceanic spreading ridges (Barberi and Varet, 1977).

The Tendaho graben exposes a thick succession of basalt flows of Pliocene age (known as the Afar Stratoid Series) at its borders. The graben is filled with thick lacustrine and alluvial deposits consisting of siltstone and sandstone. Very young basaltic flows and scoria cones (the Afar axial ranges) have been emplaced on top of the graben volcanoclastic sediments. The axial zone is also characterised by the presence of open fissures and numerous active faults which as a whole define the sites of active spreading.

The fissures and faults are evidence of active and fossil hydrothermal deposits which extend for several kilometres along strike. In fact, the most interesting feature of this area is the extensive hydrothermal activity which is controlled by NW-SE trending normal faulting. In the Tendaho rift, the hydrothermal activity in the area extends for several kilometres following a general NW-SE trend and consists mainly of steaming grounds. Several veins preferably cut the rocks undergoing potassic alteration. These veins, with variable strike between NW-SE, range from veinlets a few metres long and a few centimetres thick to bodies several hundreds of metres long. The quartz forming in these veins may be chalcedony near the walls, but commonly the central part of the veins is crystalline and colourless. The alteration is manifested by the presence of mineral assemblages including chlorite, smectite, vermiculite, epidote, adularia and quartz. The sulphide minerals include pyrite, galena, chalcopyrite, stibnite and covellite (Aqater, 1996).

### ***Petrological notes on the analyzed samples***

According to descriptions by several workers Di Paola (1972), Peccerillo *et al.* (1995), Giday Woldegabriel *et al.* (1990), the volcanic rocks of the above described formations range in composition from alkali olivine basalts to peralkali rhyolite and have the following general petrographic features:

### *Ignimbrites*

These rocks show a remarkable uniformity of composition over large areas. They are porphyritic peralkaline rhyolites with abundant glassy matrix usually constituted by a very fine glassy dust. The common phenocrysts are anorthoclase, acmite and fayalite. Lithic fragments are abundant in the ignimbrites.

### *Peralkaline rhyolite*

These rocks are represented by lava flows, lava domes and pumice falls and flows. Petrographically, they appear to be always highly glassy, with variable contents of the following minerals: alkali feldspar, generally anorthoclase, acmite, alkali amphibole (riebeckite) and rare fayalite and quartz.

### *Basalts*

In the studied area, the basalts are usually holocrystalline and they show typical features of transitional basalts with alkaline affinity. The mineralogical assemblage is the following: magnesian olivine, clinopyroxene of augite type, calcic plagioclase, magnetite, ilmenite and rare small apatite crystals.

At Tendaho, the sedimentary sequence in which TD1 core samples were recovered consists of mainly brown to light brown siltstones and grey to greenish-grey, sometimes laminated siltstones with variable calcareous component and fine-grained matrix. Basalts, belonging to the Axial Ranges and those belonging to the Afar Stratoid series show moderately porphyritic intergranular/sub-oplytic texture. The phenocrysts include: olivine, clinopyroxene sometimes titaniferous and basic plagioclase (labradorite).

## **ANALYTICAL METHOD AND RESULTS**

A total of 579 core and cutting samples were analyzed for gold by ICP-MS method at the University of Cagliari, Italy. The applied analytical method is a modification of that proposed by Gowing and Potts (1991). The following modification was found useful for a first rapid screening of samples. Twenty millilitre of freshly prepared aqua regia was added to the powdered sample ( $10.0 \pm 0.1$  g) in a 500 ml graduated Erlenmeyer flask. The flask was covered with a watch glass and the mixture stirred on a magnetic stirring table (15 positions) for 30 minutes at room temperature. The mixture was diluted to

volume after addition of 50 ppb of Indium as an internal standard and filtered (20 ml) for ICP-MS gold determination.

The detection limits were calculated at ten times the standard deviation of the blank (11 replicates) divided by the sensitivity and multiplied by the dilution factor (50), which was about 2 ppb.

The precision of the analytical method was evaluated at two different Au concentration levels by leaching two samples, subjected to 11 replicates both (Table 1).

**Table 1. Gold concentration levels subjected to replicates.**

	Sample 1	Sample 2
Average	240 ppb	11 ppb
Standard Deviation	6.6 ppb	1.6 ppb
Relative standard deviation	2.74%	14,6%

Analytical accuracy was assessed by comparison of the results obtained with the certificate of analysis for two Reference Standard Materials (Table 2).

**Table 2. Comparison of results with analysis of reference standard materials.**

Reference material	Au certified	Au found	relative error	No of replicates
Gold Ore MA-2	1860 ppb	1890 ppb	1.6%	3
Platinum ore SARM-7	310 ppb	319 ppb	2.9%	3

Analytical results obtained in this work are partly presented in Table 3. Analyses of a total of 579 core and cutting samples collected from 18 deep holes from the studied localities showed gold contents that range from hundreds of ppb to 440 ppb (Table 3). Concentrations ranging from 120 to 300 ppb are very common throughout the geological profiles particularly at Corbetti and Gedemsa calderas and Tendaho graben. Gold content, although irregular or erratic, commonly exceeds 150 ppb both in compact rocks and in pumice

fragments at Corbetti. At Gedemsa caldera, gold content ranges from 100 to 440 ppb. On Aluto volcano, gold value ranges from few ppb to 140 ppb while analysis of a sample from a core at Tendaho (TD1) range in value from 100 to 200 ppb Au.

The mean gold content from the above localities exceeds the maximum gold values reported in Boyle (1979; 1987): 3 ppb for rhyolite; 5 ppb for the upper lithosphere. Nearly all the analyzed samples showed high anomalous values starting from a depth of four metres downwards.

**Table 3. Gold concentrations (in drilled cores and cuttings) at CTG (Corbetti caldera), GDH (Gedemsa caldera), LA (Aluto volcano) and TD (Tendaho graben).**

No.	Label	Depth(m)	Au (ppm)	Lithology
275	CTG -7	27	166	rhyolite lava
276	CTG -7	30	257	rhyolite lava
277	CTG -7	43	295	rhyolite lava
278	CTG -7	49	155	rhyolite lava
279	CTG -7	52	404	rhyolite lava
280	CTG -7	55	61	pumiceous ignimbrite
281	CTG -7	58	10	pumiceous ignimbrite
282	CTG -7	64	234	pumiceous ignimbrite
283	CTG -7	67	86	pumiceous ignimbrite
284	CTG -7	69	262	pumiceous ignimbrite
285	CTG -7	72	51	basic tuff
286	CTG -7	75	12	basic tuff
287	CTG -7	78	133	basic tuff
288	CTG -7	81	287	basic tuff
289	CTG -7	84	13	rhyolite lava
290	CTG -7	87	90	rhyolite lava
291	CTG -7	90	10	rhyolite lava
292	CTG -7	93	62	rhyolite lava
293	CTG -7	96	142	lake sediment
294	CTG -7	99	108	lake sediment
295	CTG -7	102	287	lake sediment
296	CTG -7	105	118	basalt with thin rhyolite
297	CTG -7	11	74	basalt with thin rhyolite



**Table 3. (Contd).**

No.	Label	Depth(m)	Au (ppm)	Lithology
298	CTG -7	114	86	basalt with thin rhyolite
299	CTG -7	135	107	basalt with thin rhyolite
300	CTG -7	138	158	basalt with thin rhyolite
301	CTG -7	141	11	basalt with thin rhyolite
302	CTG -7	144	70	basalt with thin rhyolite
303	CTG -7	147	236	basalt with thin rhyolite
304	CTG -7	158	55	basalt with thin rhyolite
305	CTG -7	162	34	basalt with thin rhyolite
306	CTG -7	174	140	basalt with thin rhyolite
307	CTG -7	177	208	basalt with thin rhyolite
308	GDH -1	6	178	Alluvium
309a	GDH -1	9	61	Alluvium
309b	GDH -1	9	ND	Alluvium
310	GDH -1	21	272	pumiceous breccia
311	GDH -1	28	143	rhyolite lava
312	GDH -1	31	99	rhyolite lava
313	GDH -1	34	46	Basalt lavas
314	GDH -1	40	28	Basalt lavas
315	GDH -1	49	210	Basalt lavas
316	GDH -1	55	58	Basalt lavas
317	GDH -1	58	101	Basalt lavas
318	GDH -1	67	56	Basalt lavas
319	GDH -1	73	161	Basalt lavas
320	GDH -1	82	99	pumiceous ignimbrite
321	GDH -1	88	146	pumiceous ignimbrite
322	GDH -1	97	173	pumiceous ignimbrite
323	GDH -1	97-100	172	pumiceous ignimbrite
324	GDH -1	121	99	pumiceous ignimbrite
325	GDH -1	130	45	pumiceous ignimbrite
326	GDH -1	139	232	pumiceous ignimbrite
327	GDH -1	145	130	pumiceous ignimbrite
328	GDH -1	154	110	pumiceous ignimbrite
329	GDH -1	157	106	pumiceous ignimbrite
330a	GDH -1	163	142	pumiceous ignimbrite
330b	GDH -1	163	64	pumiceous ignimbrite
331	GDH -1	172	131	pumiceous ignimbrite

**Table 3. (Contd).**

No.	Label	Depth(m)	Au (ppm)	Lithology
332	GDH -1	181	57	pumiceous ignimbrite
333	GDH -1	184	98	pumiceous ignimbrite
334	GDH -2	6	56	Alluvium
335	GDH -2	9	266	Alluvium
336	GDH -2	30	312	pumiceous breccia
337	GDH -2	36	165	pumiceous breccia
338	GDH -2	39	215	pumiceous breccia
339	GDH -2	45	195	pumiceous breccia
340	GDH -2	51	177	pumiceous breccia
341	GDH -2	60	77	rhyolite lava
342	GDH -2	63	116	rhyolite lava
343	GDH -2	69	97	Basalt lavas
344	GDH -2	72	155	Basalt lavas
345	GDH -2	75	110	Basalt lavas
346	GDH -2	87	95	pumiceous ignimbrite
347	GDH -2	90	97	pumiceous ignimbrite
348	GDH -2	96	90	pumiceous ignimbrite
349	GDH -2	102	109	pumiceous ignimbrite
350	GDH -2	108	56	Basalt lavas
351	GDH -2	111	95	Basalt lavas
352	GDH -2	114	56	Basalt lavas
353	GDH -2	120	235	Basalt lavas
354	GDH -2	123	214	Basalt lavas
355	GDH -2	129	75	Basalt lavas
356	GDH -2	138	45	pumiceous ignimbrite
357	GDH -2	141	182	pumiceous ignimbrite
358	GDH -2	144	131	pumiceous ignimbrite
359	GDH -2	147	187	pumiceous ignimbrite
360	GDH -2	150	145	pumiceous ignimbrite
361	GDH -2	152	46	pumiceous ignimbrite
362	GDH -2	156	51	rhyolite lava
363	GDH -2	159	12	rhyolite lava
364	GDH -2	162	302	rhyolite lava
365	GDH -2	165	250	rhyolite lava
366	GDH -2	168	141	rhyolite lava
367	GDH -2	171	83	rhyolite lava

**Table 3. (Contd).**

No.	Label	Depth(m)	Au (ppm)	Lithology
368	GDH -2	177	105	rhyolite lava
369	GDH -2	180	103	rhyolite lava
370	LA-2	1250-1253	135	Bofa basalt
371	LA-6	2200-2203	144	rhyolite lava
372	LA-4	615-617	79	Unconsolidated ash
373	LA-7	550-554	85	Lithic tuff
374	LA-2	1600-1601	107	Bofa basalt
375	TD-1	805-808	118	Basalt lava
376	TD-1	1550-1551	117	Basalt lava
377	TD-1	1588-1597	223	Basalt lava
378	TD-1	1600-1650	108	Basalt lava
379	TD-1	1755-1800	204	Basalt lava
380	TD-1	1855-1900	108	Basalt lava
381	TD-1	1900-1950	200	Basalt lava
382	TD-1	1955-2000	129	Basalt lava
383	TD-1	2009-2017	179	Basalt lava
384	TD-1	2055-2100	156	Basalt lava
385	TD-1	2105-2150	149	Basalt lava

ND, no data.

## DISCUSSION

The results reported in this work represent the first phase of studies on epithermal occurrences within the main Ethiopian Rift (MER) and Afar. Much work has to be done in order to arrive at a reasonably well-documented synthesis. However, a working hypothesis can be attempted as a basis for future detailed studies from the obtained observations and results. The different associations among ore mineral paragenetic assemblages and alterations seem to reflect different levels of mineralization. This is shown at Corbetti and Gedemsa which are hosted in similar volcanic systems. At Corbetti the occurrence of base metals is accompanied essentially by propylitic alteration, while at Gedemsa, precious metals and quartz adularia occur, in association with potassic and argillic alterations. Thus the low sulphidation type occurrences are in good agreement with proposed schemes for epithermal mineralization

(*e.g.*, Hollister, 1985; Heald *et al.*, 1986). Furthermore, the fact that the mineralization is intimately related to potassic alteration is similar to that described by Sander and Einaudi (1990) for Round Mountain, Nevada.

Gold most probably originates from Precambrian basement, which is presumed to extend under the rift floor. Hydrothermal fluids rise through a network of fractures found within and outside the caldera, provided that a major fracture system is present that should serve as a plumbing system.

In the Corbetti caldera, one possible source of the fluids may have been the two rhyolite domes near the road just north of the steaming ground structure which apparently represent an intersection between the N-S fault structure (Fig. 2) and a contact between pyroclastic and hard, impervious compact rocks. This fluid channel way is marked by the abundant silica in crustation of the surfaces. Other similar structures capable of driving solutions might exist that potentially localize sites of gold enrichment. Irregular fracture systems within the caldera cause sporadic alteration and variable gold values in the same rock unit. The youngest pumice unit appears fresh (except where fractures offer reactive channels, *e.g.*, steaming ground area), although the gold content is comparable to that of the underlying rocks. This may have resulted from the almost neutral fluid because buffered by alkalis in underlying rocks, but still containing gold, permeated through the interface of rock pumice and spread through the unconsolidated, highly permeable material such as pumice. A further expansion, resulting in an adiabatic drop in pressure and temperature would enhance the precipitation of gold from the circulating solution. Mixing with surface water might also occur, that recharges the ground water body which occurs along the interface between the pumice-hard rock. The high precipitation characterising the area, the high permeability of the surface and the low permeability of the underlying rocks all favour this model. The wide surface area offered by the pumice and its glassy nature, allow adsorption phenomena in the entire pumice unit.

As far as the age of epithermal mineralization in the rift is concerned, no quantitative data are yet available. However, it has been established that in all areas, where gold occurrence has been documented, the host rocks are ignimbrites, rhyolite lavas and pumice deposits, with subordinate basaltic rocks. Thus, the epithermal occurrences are mostly hosted in acidic rocks emitted from central volcanoes during Late Quaternary times, *i.e.*, younger than 0.8 Ma.

The overall characteristics of the known occurrences and the evolution of the central volcanoes within the rift and the associated epithermal phenomena apparently define an individual, homogeneous metallogenic province within the rift. Obviously, it is too early to give any economic evaluation, but the field and analytical data appear encouraging for the development of exploration and a preliminary estimate for gold, at least in the Corbetti, Gedemsa and Tendaho prospects.

For instance, taking an average value of 100 ppb for the gold dispersed in the upper uniformly spread unwelded pumice unit having an average thickness of 40 m over a surface area of 50 km<sup>2</sup>, the total reserve (assuming a specific gravity of 0.9 for pumice) can be calculated to over 200 tons in just one of the calderas alone, *i.e.*, a gold reserve level of an important mine.

At current mining exercise, 0.1 g/t average gold content is too low for the wide pumice layer to be considered as economical. It is to be noted, however, that neither the bore holes used for the present evaluation were strategically located to intersect known fluid driving structures nor was it possible to have fully representative composite core samples for assay. If systematic geophysical and exploration drilling directed for gold were done, the subsequent analysis may enable to identify high grade gold concentration target areas even at shallow depth.

As a conclusion, this is the first indication of epithermal gold resources in the Ethiopian rift and this might be an important new target for exploration. The situation of East African rifts, not yet considered as a possible site for this kind of mineralization, should be carefully assessed. A fascinating field of mineral prospecting can be envisaged in these wide volcanic areas of Ethiopia and other East African countries.

#### ACKNOWLEDGEMENTS

This research was funded by the Ethio-Italian University Cooperation Programme. Special thanks are to the Ethiopian Institute of Geological Survey which provided the necessary data pertinent to the present study. The author is especially indebted to Professor S. Pretti of the University of Cagliari, Italy, and Dr Gezahegn Yirgu, Department of Geology and Geophysics, AAU, for the many thorough, scholarly

discussions on earlier versions of the manuscript. Special thanks are also to Alessandro Rivoldini of the University of Cagliari, Italy for analysing all the samples.

## REFERENCES

1. Aquater (1996). Tendaho Geothermal Project, final report. Aquater, Italian Ministry of Foreign Affairs, Vol. 1, pp. 1–44.
2. Barberi, F. and Varet, J. (1977). Volcanism of Afar: Small-scale plate tectonic implications. *Bull. Geol. Soc. Amer.* **88**:1251–1266.
3. Boyle, R.W. (1979). *The Geochemistry of Gold and its Deposits*. Canada, pp. 280–584.
4. Boyle, R.W. (1987). *Gold: History and Genesis of Deposits*. Ottawa, Ontario, Canada.
5. Burke, K.C., Kidd, W.S.F., Turcotte, D.L., Dewey, J.F., Mougini-Mark, P.J., Parmentier, E.M., Sengor, A.M.C. and Tapponier, P.E. (1981). Tectonics of basaltic volcanism. In: *Basaltic Volcanism on the Terrestrial Planets*, pp. 803–898. Lunar and Planetary Inst. Houston, Texas, Pergamon Press, New York.
6. Di Paola, G.M. (1972). Geology of the Corbetti caldera area (Main Ethiopian Rift). *Bull. Volcanol.* **35**:497–506.
7. ELC (1986). Exploitation of Langanò-Aluto geothermal resources. Electroconsult (ELC), Feasibility report. Milano, Italy.
8. Giday Woldegabriel, Aronson, J.L. and Walter, R.C. (1990). Geology, geochemistry and rift basin development in the central sector of the Main Ethiopian Rift. *Bull. Geol. Soc. Amer.* **102**:439–458.
9. Gianneli, G. and Meseret Teklemariam (1993). Water-rock interaction processes in the Aluto-Langanò geothermal field (Ethiopia). *Jour. Volcano. Geotherm. Rese.* **56**:429–445.
10. Gowing, C.J.B. and Potts, P.J. (1991). Evaluation of a rapid technique for the determination of precious metals in geological samples based on a selective aqua regia leach. *Analyst* **116**:773–779.
11. Hatris, N.B.W., Pearse, J.A. and Tindle, A.G. (1986). Geochemical characteristics of collision zone magmatism. *Geol. Soc. Spec. Publ. No. 19*. Blackwell, London, pp. 67–81.
12. Heald, P., Hayaba, D.O. and Foley, N.K. (1986). Comparative anatomy of volcanichosted epithermal deposits: Acid-sulphate and Adularia-sericite types. *Econ. Geol.* **82**:1–26.

- 
13. Hollister, V.F. (1985). Models of precious metal epithermal deposits. **In:** Discoveries of Epithermal Precious Metal Deposits, pp. 9–14, (Hollister, V.F., ed.), Society of Mining Engineers, New York.
  14. Peccerillo, A., Gezahegn Yirgu and Dereje Ayalew (1995). Genesis of acid volcanics along the Main Ethiopian Rift - A case history of the Gedemsa volcano. *SINET: Ethiop. J. Sci.* **18**:23–50.
  15. Sander, M.V. and Einaudi, M.T. (1990). Epithermal deposition of gold during transition from propylitic to potassic alteration, Round Mountain, Nevada. *Econ. Geol.* **85**:285–311.
  16. Solomon Kebede (1987). Stratigraphy and results of temperature measurement in shallow drill holes at Corbetti caldera. Preliminary report. Geothermal Exploration Project, Ethiopian Institute of Geological Surveys.